Hindawi
Advances in Materials Science and Engineering
Volume 2024, Article ID 7961951, 14 pages
https://doi.org/10.1155/2024/7961951

Research Article

A Practical Swelling Constitutive Model of Anhydrite and Its Application on Tunnel Engineering

Jianxun Wu,[1,2] Fei Lin,[3,4] Xiaohong Zhou,[4] Zhigang Zhang,[4] Jinyang Fan,[2] and Zhenkun Hou[5]

[1]*East China Electric Power Design Institute Co., Ltd. of CPECC, Shanghai 200063, China*
[2]*State Key Laboratory for Coal Mine Disaster Dynamics and Control, Chongqing University, Chongqing 400044, China*
[3]*School of Resources and Safety Engineering, Chongqing University, Chongqing 400030, China*
[4]*China Coal Technology Engineering Group Huaibei Blasting Technology Research Institute Limited Company, Huaibei 235000, China*
[5]*School of Civil and Transportation Engineering, Guangdong University of Technology, Guangzhou 510006, China*

Correspondence should be addressed to Zhenkun Hou; zhenkunhoucqu@163.com

Received 25 June 2022; Revised 4 August 2022; Accepted 18 August 2022; Published 14 March 2024

Academic Editor: Ivan Giorgio

Swelling of anhydrite rock causes serious damage to the tunnel and generates high additional costs in the process of tunnel construction and operation and has gradually become one of the main factors that threaten the safety of the tunnel. It is extremely difficult to predict swelling pressures and deformations accurately based on conventional swelling constitutive models. Thus, a new practical swelling constitutive model of anhydrite for tunnel engineering has been developed. First, swelling tests of natural anhydrite samples focusing on the time effect have been designed and conducted, whose test results show that swelling strain-time can be described by the S-curve model and that swelling stress-strain can be described by the quadratic model. Second, a swelling constitutive model with considering the time effect has been developed to reproduce the swelling behavior of anhydrite observed in swelling tests. This model can track the evolution of swelling activity in tunneling, which has practical significance for process simulation and process control of swelling disaster. Then, this model has been implemented within ANSYS for numerical simulation of the Lirang tunnel. Based on simulation results, useful measures have been proposed. Satisfactory results have been achieved according to the feedback from the site.

1. Introduction

Anhydrite rock is a kind of widely distributed rock; with the high-speed development of the transportation industry, its negative impacts on tunnel engineering are reported increasingly, especially in China [1–3]. Its main composition $CaSO_4$ will transform into $CaSO_4{\cdot}2H_2O$ after meeting water, resulting in an increase of the solid volume by some 61%, and major swelling deformation will occur. During the construction of anhydrite rock tunnel, swelling will cause engineering disasters, such as floor heave, beyond limit or destruction of lining, and collapse of surrounding rock [1, 4]. So the swelling of anhydrite rock is a major threat in tunnel engineering and can cause serious damage to tunnels, which will produce high additional costs.

Research on engineering disaster caused by anhydrite rock in the construction of anhydrite rock tunnel can be triggered in the early 1970's. Luo [5] carried out research on swelling deformation of anhydrite rock samples and accumulated some valuable test data. Rauh et al. [6, 7] conducted some research related to the micromechanism of anhydrite swelling, while Sch¨adlich et al. [8] paid attention to a macroscopic swelling constitutive model. Microscopic swelling models based on mineral transformations in the

anhydrite-gypsum-water system were studied by Anagnostou et al. [9], Ramon Tarragona [10], and Oldecop and Alonso [11]. Alonso et al. [12] and Berdugo [13] also carried out many on-site research works including monitoring and analysis of inverted arch of tunnel. In the abovementioned literature, the swelling process of rock and soil involves the reaction of $CaSO_4$ and water to crystallize and has the characteristics of long swelling duration. Therefore, these long-lasting and chemically reactive expansive rocks can be classified into one category and can be treated differently from other clay-type expansive rocks. Based on the above research results, a great amount of practical experience and experiment research has been gained in the last decades, but tunneling in anhydrite is still a very challenging task. Reliable prediction of swelling pressures and deformations based on conventional swelling constitutive models is extremely difficult for the following reasons:

(a) The anhydrite swelling process can last a very long time. Powder samples instead of natural rock were usually employed to carry out the test for establishing the model [6, 14, 15]. For example, Liu et al. [14] used disk-shaped samples remodeled by anhydrite powder in the swelling test and obtained the relationship between the swelling stress and moisture. Actually, the models based on test results of powder samples cannot accurately reflect swelling behavior, for the structure of the powder sample is different from that of natural rock.

(b) Most constitutive models for swelling rock employ Grob's swelling law [16]. These models were established based on an underlying assumption that the relationship between swelling stress and swelling strain is stable and unchangeable in the whole swelling process. In addition, the swelling stress-strain relationship described by these models usually is under the condition of complete swelling. So, these models are only able to predict a final swelling behavior of surrounding rock but unable to track the evolution of swelling activity in tunneling. Due to the slow evolution of swelling deformations in anhydrite, the dynamic changing of swelling stress-strain before complete swelling cannot be neglected.

(c) Conventional swelling constitution models for swelling rock are usually employed by the logarithmic function to fit test data of swelling stress-strain. In the interval that swelling stress is large, the function fits the data well [17].

As the above reasons, a practical swelling constitutive model of anhydrite, considering the dynamic changing of swelling stress-strain, is the key to solve tunnel engineering problems associated with anhydrite swelling. For reason (a), we employed natural anhydrite rock samples coring from the Lirang tunnel to carry out the experiment study aiming to get closer to on-site swelling performance. For reason (b), we introduced the time effect into the swelling constitutive model; i.e., the relationship between swelling stress and strain changes over time. The time factor was taken into consideration in the test method with the aim of obtaining swelling stress-strain curves at different points in time. For reason (c), we employed a new function instead of a traditional logarithmic function to fit swelling stress-strain data.

2. Swelling Test

2.1. Sample Preparation. In order to carry out swelling tests, anhydrite rocks belonging to Lower Triassic Jialing River Group were obtained from the Lirang tunnel located in Liangping county, Chongqing, China. As shown in Figure 1(a), the results of X-ray diffraction qualitative analysis show that the compositions of anhydrite samples are $CaSO_4$, $CaSO_4{\cdot}2H_2O$, SiO_2, Fe_2O_3, and $CaCO_3$, respectively. As shown in Table 1, a quantitative analysis was carried out to determine the content of $CaSO_4$, and $CaSO_4{\cdot}2H_2O$ by employing the internal standard method. The $CaSO_4$ content ranges from 88% to 95%, the $CaSO_4{\cdot}2H_2O$ content ranges from 2% to 8%, and the content of other composition (including SiO_2, Fe_2O_3, and $CaCO_3$) ranges from 2% to 5%. As shown in Figure 1(b), these anhydrite rocks were processed into disk-shaped samples with 61 mm in height and 20 mm in diameter according to the recommendations of ISRM [19], whose process was performed air flushed in order to avoid an early activation of the swelling process. What needs illustration is that the expansion time of anhydrite expansive rock is relatively long, and there are relatively few examples for reference in the expansion experiment of this kind of rock. Most of the examples in existing research also refer to the old ISRM suggested methods from 1989. In order to have a better comparative effect with the previous results, the experiment in this paper adopts the ISRM 1989 standard.

2.2. Swelling Test Apparatus. As shown in Figure 2, Single Lever Trigeminy High Pressure Oedometer Apparatus with a maximum capacity of 4000 kPa in the vertical direction was employed to carry out the swelling tests. Besides, TWJ Data Auto Sampling System, which can distinguish a minimum vertical deformation of 0.001 mm, was also employed to assist the swelling test. This system consists of a computer, sensor, servo, and circuit and can be linked with the oedometer apparatuses, which ensures timely recording of data.

2.3. Test Method. Swelling of anhydrite is a complicated process, which is influenced by a lot of factors. In order to establish a practical model, only the time factor is concerned in this paper. A swelling stress-strain relationship is a reflection of swelling potential of rock materials because it changes over contact time with water. It is possible to obtain a complete swelling stress-strain curve at one point in time with the method suggested by ISRM [19]. However, it is not possible to obtain a series of complete swelling stress-strain curves of a separate sample at various points in time during the swelling process, because a separate sample is unable to be reused. Thus, we employed the swelling stress-strain curves of several samples after different contact times with water instead of the swelling stress-strain curves of

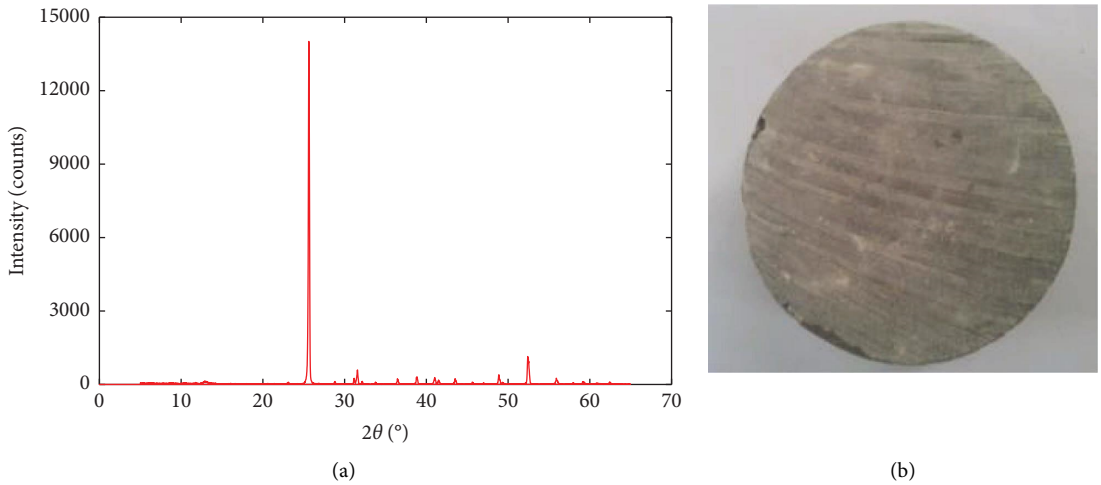

Figure 1: (a) One result of X-ray diffraction analysis. All four anhydrite samples for quantitative analysis show similar peaks as above (a). There are differences between X-ray diffraction analysis result of anhydrite in this paper and that reported by [18]. (b) An anhydrite sample after processing which is bluish-grey.

Table 1: The mineral composition of the anhydrite rock.

Sample	$CaSO_4$ (%)	$CaSO_4{\cdot}2H_2O$ (%)	Other compositions (%)
1	90	8	2
2	91	4	5
3	88	7	5
4	95	2	3

Figure 2: The left are the oedometer apparatuses linked with the data auto sampling system. The right is one of the test apparatuses. ① Computer used for indication. ② Loading frame, which can be moved away when measuring the vertical deformation without loading. ③ Dial gauge linking with the computer. ④ Water container, into which a sample is put.

a separate anhydrite sample at various points in time. The specific method is presented as follows:

(a) Free swelling test with lateral confinement (FLC): At this stage, we aimed at establishing the relationship between swelling strain and time. First, a disk-shaped anhydrite sample was embedded into a metal ring, which can be used to confine the lateral of the sample. Then, the sample with the metal was put into the water container of the oedometer apparatus. Both the top and bottom of the sample were placed on a porous plate. Then, water was poured slowly into the water container until the water surface was above the sample by 5 mm. Axial deformation was recorded by the data auto sampling system after reaching design time. Nine disk-shaped anhydrite samples were tested with the above method but different contact times with water. The swelling time of each sample is shown in Table 2.

(b) Axial swelling stress and strain test with lateral confinement (ALC): At this stage, we aimed at obtaining the swelling stress-strain relationship of the above nine samples having experienced different swelling times. After a sample finished design swelling time, the sample is put in a loading frame and loaded stepwise until the measured deformations due to swelling were compensated [19]. The compression deformation under each load was recorded, and its corresponding swelling stress-strain curve was obtained.

2.4. Test Results. Figure 3 shows the relationship between swelling strain and time from FLC. The swelling strain of all samples increases over the time. The swelling strain of No. 9 is still not finished and could continue in a constant rate after a longest swelling time 119 days. The growth rate of swelling strain of anhydrite increases initially in a positive acceleration phase and then declines in a negative acceleration phase until reaching a relatively stable positive value. The swelling process of anhydrite is a complicated physicochemical reaction. Swelling is able to be controlled by both osmotic effect of water, which is related to the speed of water inflow into the rock, and sulfate hydration, so the growth rate of swelling strain changes [20, 21]. After the rock completely contact water, the dominate reason is the sulfate hydration, whose reaction rate is relatively stable, so the swelling strain can sustain increasing with a relatively stable rate, this is why the latter part of each swelling strain-time curve is approximately an oblique line.

Table 2: The swelling time of each sample.

No	1	2	3	4	5	6	7	8	9
Swelling time (days)	7	14	21	35	49	63	77	98	119

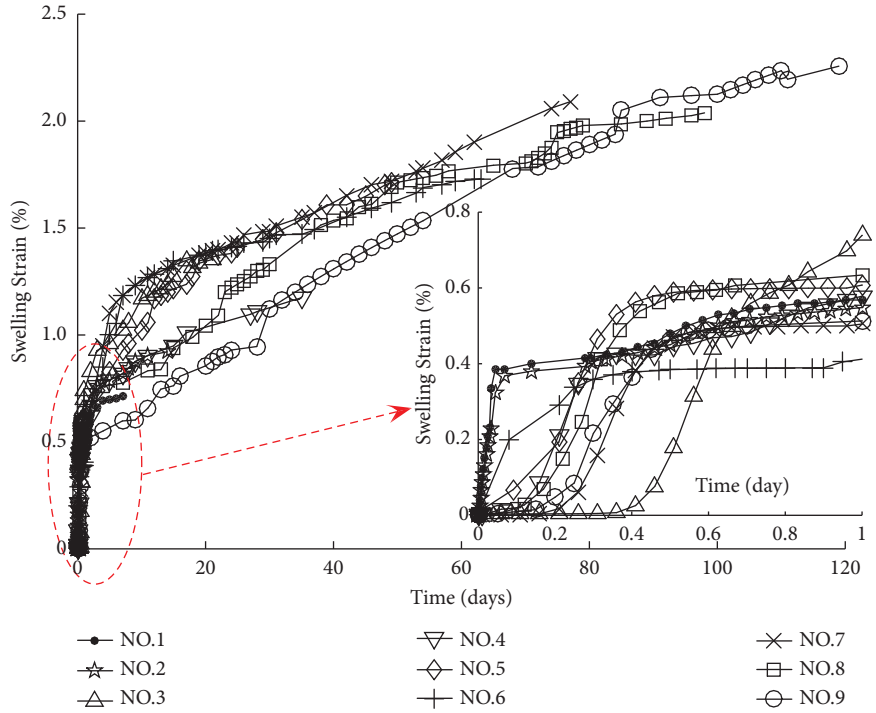

Figure 3: The relationship between swelling strain and time from free swelling with lateral confinement. The inner figure is the swelling strain-time on the first day.

Figure 4 shows the relationship between swelling stress and strain from ALC. Swelling stress is defined as the ratio of the force which can inhibit the swelling strain caused by the water seeped into the sample to the sectional area of the sample [22]. As shown in Figure 4, with the increase in swelling stress, the swelling strain decreases and all stress-strain curves behave as concave characteristic. The intersection of each curve with a swelling strain axis, which is the swelling strain of the corresponding sample at the end of FLC, goes up with the increase in sample numbers. It indicates that the longer the swelling time, the larger the swelling strain. By extending the bottom of each curve, the intersection of each curve with a swelling stress axis can be obtained, which also shows an increasing trend with the sample number increase. It indicates that the swelling stress under the condition of completely inhibiting swelling strain goes up with the increasing swelling time.

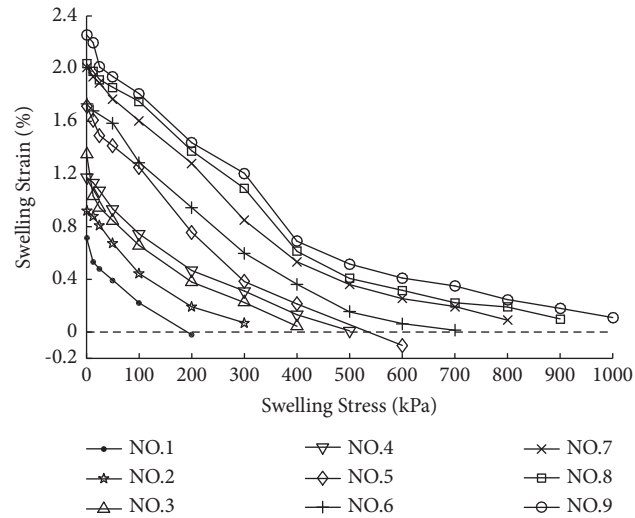

Figure 4: The relationship between swelling stress and strain from axial swelling stress and strain with lateral confinement.

3. Model Established

3.1. Swelling Strain-Time Model. As shown in Figure 5, Liu et al. employed the exponential model to describe the swelling strain-time of pure clay rock as follows [23]:

$$\varepsilon_t = \left(\frac{\varepsilon_\infty}{1 + at^{-b}}\right), \quad (1)$$

where t is the time, ε_t is the swelling strain at time t, ε_∞ is the final swelling strain, and k is the coefficient depending on characteristics of rock.

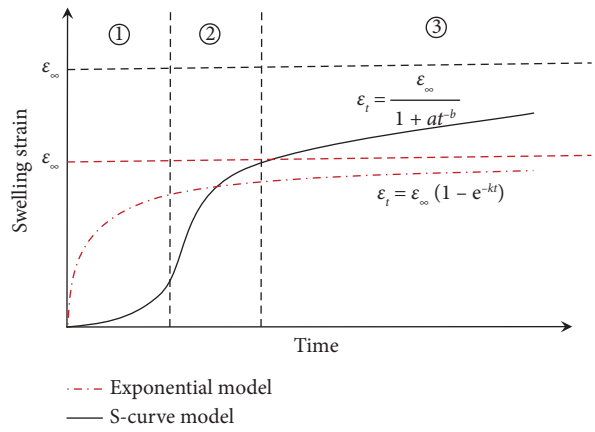

Figure 5: Introduction of two kinds of swelling strain-time model. The red line is the exponential model employed in [23]. The black line is the S-curve model employed in this paper. In the representation of the S-curve model, there are three clearly defined phases: ① the growth rate of swelling strain increases over time. This phase can be very short, for example, the data of No. 1 and No. 2 samples in Figure 3. ② Swelling strain increases rapidly, while the growth rate of it decreases over time. ③ The increase of swelling strain is relatively stable and is able to last a long time and will be close to a maximal swelling strain too. ① and ② Unstable phases of the growth rate of swelling strain, which is controlled by the combined effect of both the osmotic effect and hydration effect. ③ A relatively stable increase phase of swelling strain, of which the hydration effect is dominant.

This model is able to describe the swelling stress-time of pure clay rock well but not for anhydrite rock. It cannot describe the changing process of the growth rate of swelling strain, which is controlled by the coupled effect of both the osmotic effect and hydration effect, before the water is in full contact with rock. Although such a changing process lasts a short time in the laboratory test, it can last a long time in the field test [2]; i.e., the changing process will be more obvious with increasing the size of the rock sample. Such a long duration of the changing process has an impact on tunnel construction and design. Second, this model cannot describe well the relatively stable status of the growth rate of swelling strain after water is in full contact with rock, which is very important for predicting the final swelling deformation in tunnel engineering.

Thus, we employed an S-curve model, which has been widely used to show the growth rate of a variable changed over time [24], to describe the swelling strain-time due to the fact that the curve of each sample in Figure 3 is approximately S-shaped. The model is as follows:

$$\varepsilon_t = \left(\frac{\varepsilon_\infty}{1 + at^{-b}} \right), \tag{2}$$

where a and b are coefficients related to characteristics of rock. In this equation, if time tends to infinity, ε_t will tend to a maximal swelling strain ε_∞. It indicates that swelling strain is not able to increase to infinity but has an upper limit. This agrees with the practical situation, and several papers ([6, 25]) point out that the upper limit, i.e., maximal swelling strain ε_∞, of pure anhydrite is 61%. Actually, 61% is an ideal value and is never obtained in the test. So, in the practical application of this model, ε_∞, just as a coefficient, should be obtained by fitting the test data.

Theoretically, the higher the main component $CaSO_4$ in anhydrite, the more components in the anhydrite can participate in the expansion reaction to produce a greater final expansion strain. In formula (2), the meaning of ε_∞ is the final expansion strain and should have a quantitative relationship with the content of the main component $CaSO_4$. In order to improve the constitutive model, we will conduct further research to clarify this quantitative relationship.

As shown in Figure 6, for a better comparison, we fitted the nine sample data by using the two swelling strain-time models, respectively. It is obvious that the S-curve model is better than the exponential model for anhydrite rock swelling strain-time; especially, it can better describe the continuing increase process of swelling strain. Table 3 is the summary fits of swelling strain-time of nine samples for the two models. In terms of a separate sample, the R-squared of the S-curve model is higher than that of the exponential model, which also indicates the S-curve model is better than the exponential model. It should also be noted that a maximal swelling strain ε_∞ estimated by the S-curve model is more than that by the exponential model.

3.2. Swelling Stress-Strain Model. As shown in Figure 7, based on the laboratory test of clay rocks, Einstein et al. [26–28] formulated a logarithmic model to describe the swelling stress-strain:

$$\varepsilon = K \left[1 - \frac{\lg(\sigma)}{\lg(\sigma_m)} \right], \tag{3}$$

where ε is the swelling strain at a given axial stress σ (i.e., swelling stress based on definition) and K and $\lg(\sigma)$ are coefficients depending on the rock features. As shown in Figure 7, the intersection of the logarithmic curve with the stress axis supplies the coefficient σ_m. For stresses σ larger than σ_m, no more swelling strains occur. For small stresses, the application scope of the swelling law is limited by minimum stress, because unrealistically high swelling strains would result otherwise. Furthermore, very small stresses lead to decomposition processes in the rock, which cannot be described by the swelling law [27].

For this problem, as shown in Figure 4, we employed the left part of a parabola opening upwards, the vertex of which is on the X-axis, to describe the swelling stress-strain due to the curve feature of each sample. As shown in Figure 7, this model is a quadratic function and has intersections with both the X-axis and Y-axis:

$$\varepsilon = p(\sigma - \sigma_m)^2, \tag{4}$$

where ε is the swelling strain, σ is the swelling stress, and p and σ_m are coefficients depending on the feature of rock. In terms of a separate sample, σ_m is the swelling stress under swelling strain inhibited completely, while $p\sigma_m$ is the swelling strain without inhibiting.

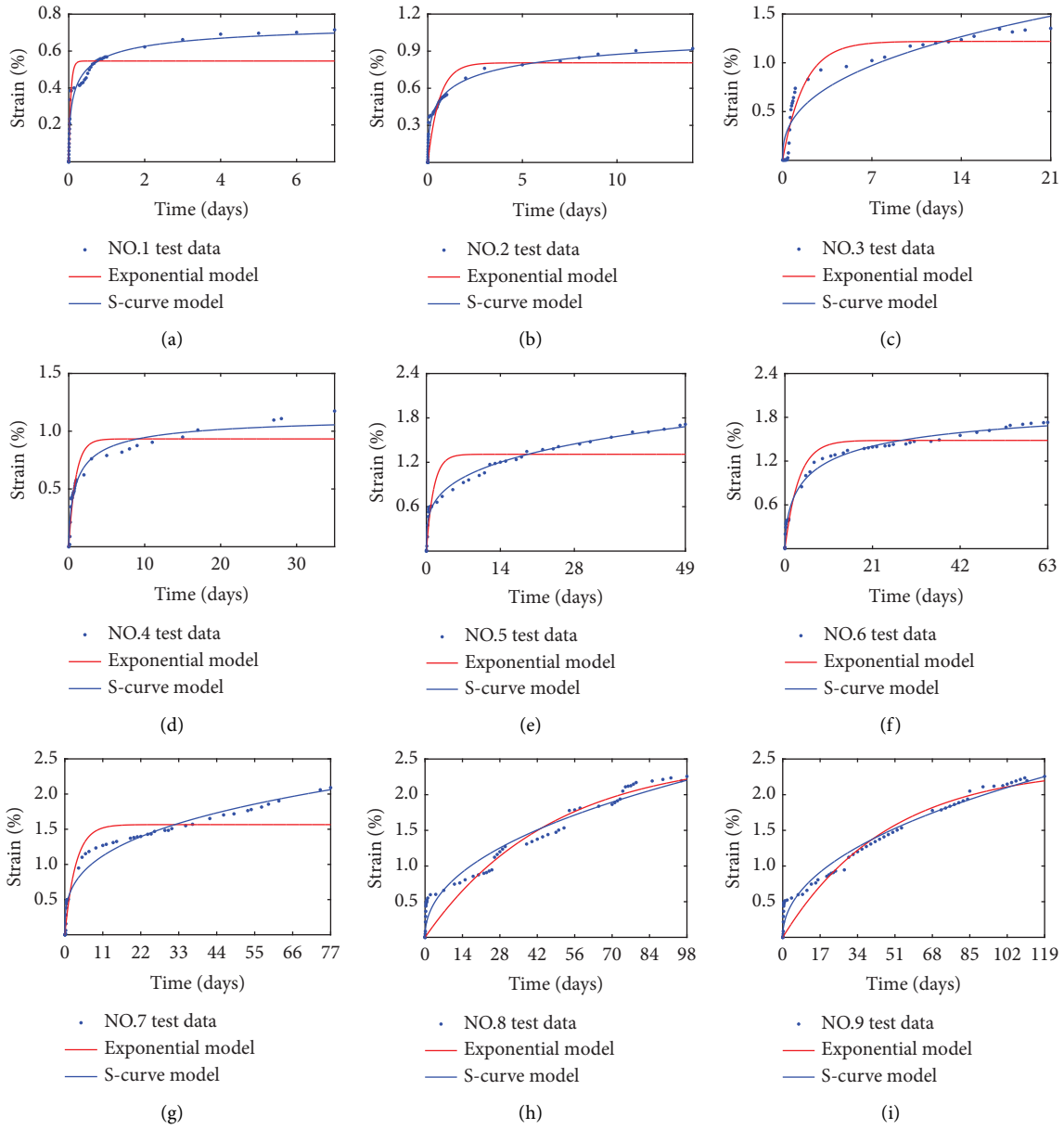

Figure 6: Swelling strain-time fitting results of nine samples of the exponential model and the S-curve model, respectively.

Table 3: Summary fits of swelling strain-time of nine samples for the exponential model and the S-curve model.

No	Exponential model: $\varepsilon_t = \varepsilon_\infty (1 - e^{-kt})$			S-curve model: $\varepsilon_t = \varepsilon_\infty/(1 + at^{-b})$			
	ε_∞	k	R-square	a	b	ε_∞	R-square
1	0.0055	19.000	0.9082	0.3777	0.5599	0.0079	0.9727
2	0.0081	1.6400	0.8760	1.1290	0.4658	0.0121	0.9839
3	0.0122	0.5943	0.9299	54.370	0.4014	0.2516	0.8806
4	0.0093	1.0900	0.9119	1.0990	0.7054	0.0115	0.9610
5	0.0131	0.7403	0.8310	67.230	0.2789	0.3987	0.9788
6	0.0148	0.3044	0.9412	3.2180	0.5935	0.0215	0.9923
7	0.0157	0.3184	0.9097	138.60	0.3203	0.7320	0.9653
8	0.0253	0.0214	0.9094	196.30	0.4645	0.5360	0.9533
9	0.0239	0.0211	0.9322	194.40	0.4791	0.4666	0.9708

Note. R-square is a number that indicates how well data fit a statistical model and is known as the coefficient of determination. In general, the higher the R-square, the better the model fits data. The above results were obtained using MATLAB Curve Fit Tool.

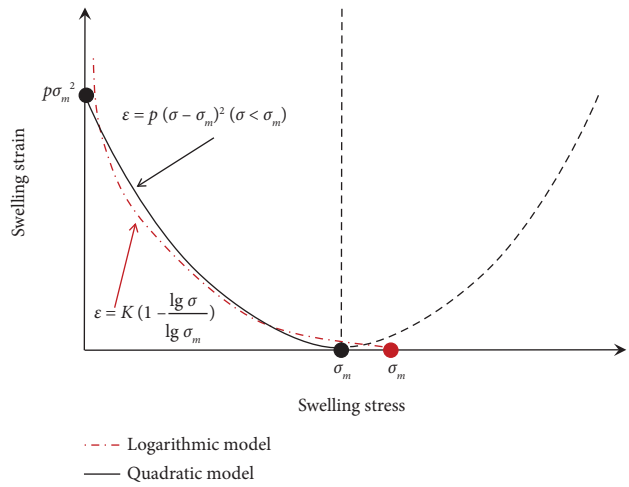

Figure 7: Introduction of two kinds of swelling stress-strain model.

As shown in Figure 8, for comparison, we fitted the data of swelling stress-strain by using the two models, respectively. It is obvious that the quadratic model is better than the logarithmic model for anhydrite rock swelling stress-strain, especially in the interval that swelling stress is small. Table 4 is the summary fits of swelling stress-strain of nine samples for the two models. The most R-square of the quadratic model is higher than that of the logarithmic model, which also indicates the quadratic model is better.

3.3. Swelling Constitutive Model with Consideration of Time Effect. Unlike pure clay swelling rocks, the swelling of anhydrite rock is highly time-dependent [27]. Pure clay rock is able to finish swelling in several days, while anhydrite needs a very long time. In this paper, the swelling of anhydrite rock is still not finished and could continue even though swelling time is up to 119 days. Therefore, the time dependency of anhydrite swelling cannot be neglected. By disregarding the influence of the individual difference of the sample to swelling, the curve of each sample in Figure 4 can be regarded as swelling stress-strain of a separate anhydrite rock at different points in time. So, if making these data corresponds to the time, a swelling constitutive model with consideration of the time effect can be established. This model can describe a dynamic process that the swelling stress-strain curve of an individual anhydrite changes over time.

As illustrated in Section 3.2, data in Figure 4 can be better fitted with a series of parabolas. So, the dependence of swelling stress-strain on time can be established by finding out the movement history of intersections of parabolas with the axis. First, in terms of a separate anhydrite, the intersections of parabolas with the Y-axis, $\rho\sigma_m^2$ (obtained by substituting $\sigma_m = 0$ into equation (4)) represent strain from FLC, so their movement history can be better described by equation (2), that is,

$$\begin{aligned} \rho\sigma_m^2 &= \varepsilon_t \\ &= \frac{\varepsilon_\infty}{1 + at^{-b}}. \end{aligned} \tag{5}$$

Second, the intersections of parabolas with the X-axis, σ_m (obtained by substituting $\varepsilon = 0$ into equation (4)) are swelling stresses under the condition of completely inhibiting swelling strain. The relationship between σ_m of parabolas and time is shown in Figure 9. σ_m increases over time, while its increase rate tends to decrease. This is because the longer the expansion time, the smaller the infiltration rate of water in the sample, the denser the sample, and the larger the expansion stress. Previous research [29–31] also indicates that σ_m of swelling rock increases quickly at the early stage and then tends to a constant value. We employed the following equation to describe movement history of σ_m:

$$\sigma_m = \sigma_{\max}\left(1 - e^{-ct}\right), \tag{6}$$

where $\sigma_{\max}$ and c are coefficients that depend on the rock feature and $\sigma_{\max}$ is maximal $\sigma_{\max}$ (when time t tends to infinity), i.e., the swelling stress under the condition of inhibiting completely swelling strain when rock completely finishes swelling.

After finding out the movement history of intersections of parabolas with both the X-axis and Y-axis, the swelling constitutive model with consideration of the time effect can be established by substituting equations (5) and (6) into equation (4):

$$\varepsilon = \frac{\varepsilon_\infty \left[\sigma - \sigma_{\max}\left(1 - e^{-et}\right)\right]^2}{\sigma_{\max}^2\left(1 + at^{-b}\right)\left(1 - e^{-et}\right)^2}. \tag{7}$$

In this model, both time t and swelling stress σ are independent variables, while ε is the dependent variable. This model is a surface in a three-dimensional space and is

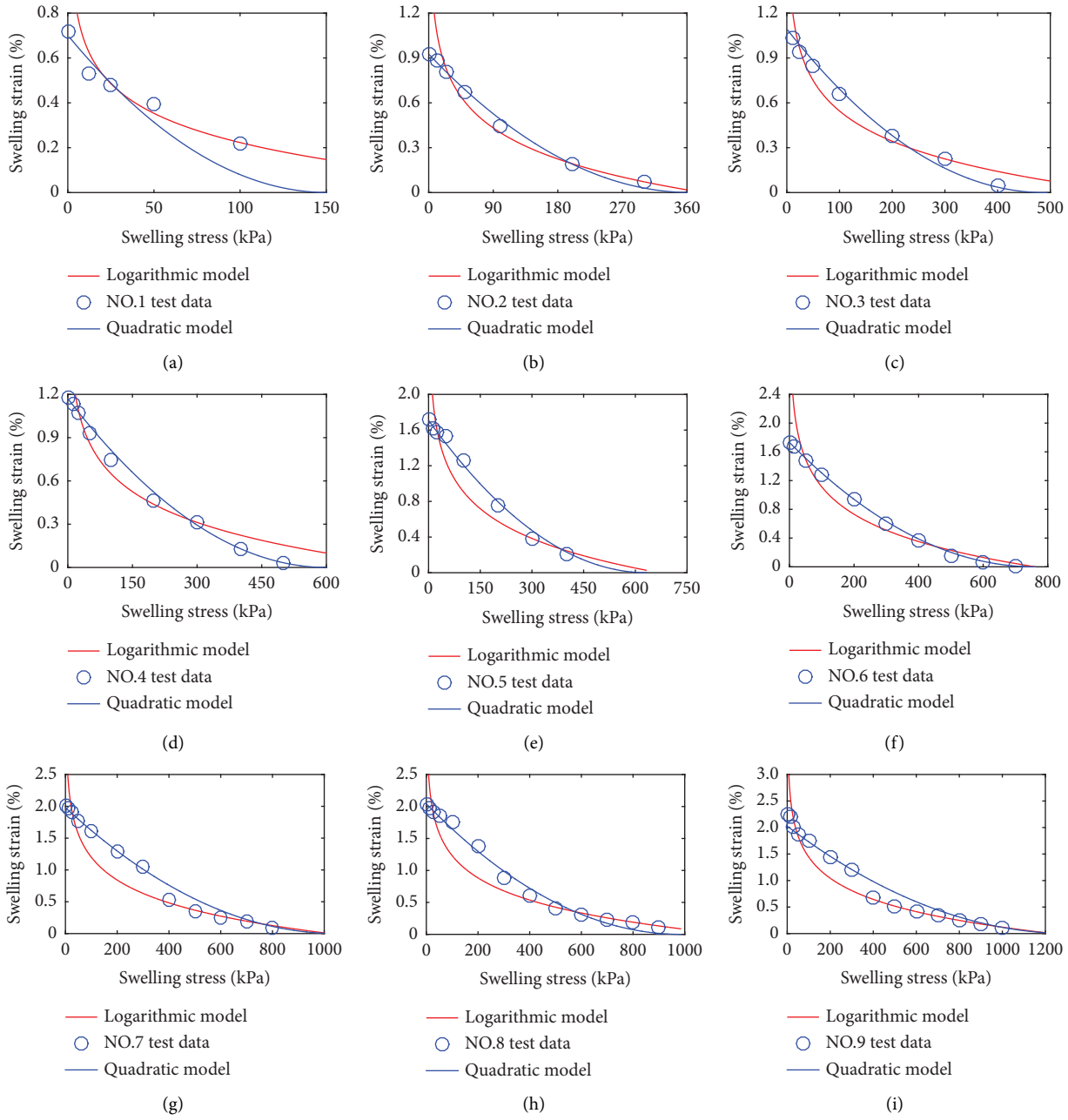

Figure 8: Swelling stress-strain fitting results of nine samples of the logarithmic model and the quadratic model, respectively.

established to describe the dynamic process that the swelling stress-strain relationship changes over time with disregarding the influence of the individual difference. As it can be regarded as the swelling stress-strain of an individual anhydrite rock at different points in time, all data in Figure 4 were fitted by this model using MATLAB sftool.

As shown in Figure 10, test data are equably distributed around the fitting surface. It indicates that this model fits the test data well. As shown in Table 5, R-square is close to 1, while both RMSE and SSE are close to 0. All of them also support the view that this model can reflect the dynamic process of swelling stress-strain of anhydrite well. It is very meaningful that the estimated value of ε_{∞} of this model, which is a final swelling strain, is close to its theoretical value of 61% [1, 32] as in pure anhydrite rock. The error between the estimated value and the theoretical value may be caused by the $CaSO_4$ content.

4. Application of the Model

This study is part of a project carried out at the Lirang tunnel in Chongqing, China. The left channel from ZK14 + 582 to ZK14 + 907 and the right channel from K14 + 599 to K14 + 920 in the Lirang tunnel go through about 300 m anhydrite-gypsum stratum. In this section, the swelling constitutive model (7) was implemented within ANSYS to

Table 4: Summary fits of swelling stress-strain of nine samples for the logarithmic model and the quadratic model.

No	Logarithmic model: $\varepsilon = K[1 - \lg(\sigma)/\lg(\sigma_m)]$			Quadratic model: $\varepsilon = p(\sigma - \sigma_m)^2$		
	σ_m	K	R-square	p	σ_m	R-square
1	329.60	0.0107	0.8989	$3.077E-7$	151.00	0.8822
2	381.30	0.0177	0.9538	$6.915E-8$	365.00	0.9940
3	650.00	0.0188	0.9327	$4.587E-8$	487.30	0.9841
4	830.00	0.0311	0.9490	$3.243E-8$	600.00	0.9937
5	668.00	0.7403	0.8796	$4.255E-8$	632.90	0.9919
6	759.80	0.0362	0.8692	$3.004E-8$	758.30	0.9988
7	1020.0	0.0357	0.8761	$1.792E-8$	1050.0	0.9840
8	1171.0	0.0352	0.8826	$2.100E-8$	985.30	0.9904
9	1233.0	0.0407	0.9815	$1.169E-8$	1315.0	0.9599

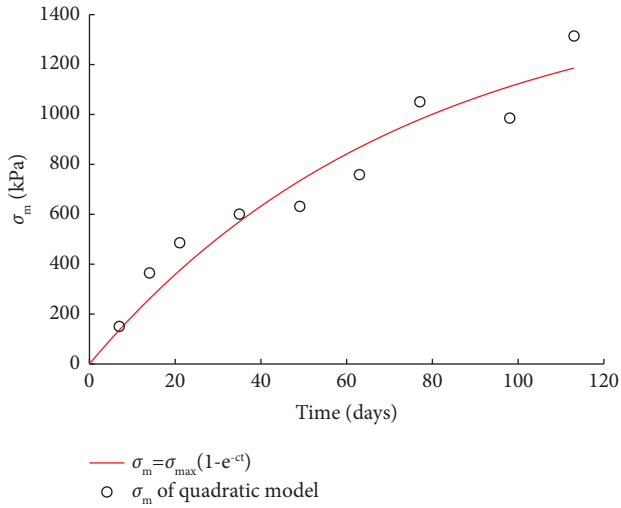

Figure 9: The relationship between σ_m of the quadratic model and time.

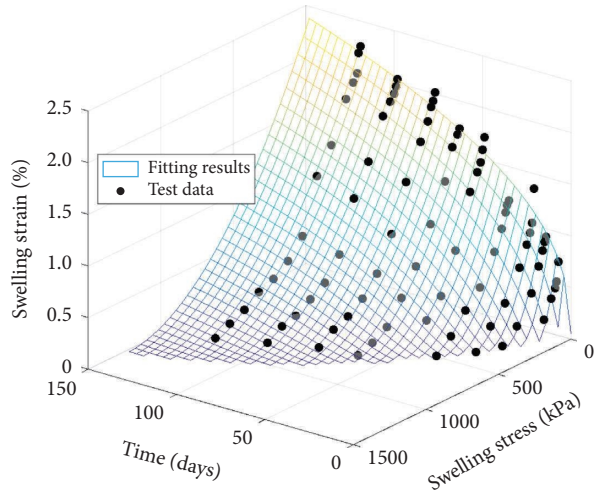

Figure 10: Comparisons between test data and prediction of the swelling constitutive model with consideration of the time effect.

simulate the influence of swelling on the tunnel during the construction period, so that some practical measures based on simulation results were proposed to counteract the swelling problem.

A previous simulation for surrounding rock swelling usually used the method of simulating thermal expansion for reference. For example, Miao et al. ever simulated swelling of surrounding rock by corresponding humidity stress field to

Table 5: Summary fits of swelling stress-strain changing over time for the swelling constitutive model with consideration of the time effect.

ε_{∞} (%)	Parameters				Goodness of fit		
	σ_{max} (kPa)	a	B	c	R-square	RMSE	SSE
52.04	1510	150.30	0.3954	0.0125	0.9750	0.0011	$9.4820E-5$

Note. Parameter ε_{∞} (%) = 52.04% indicates that swelling strain of this type anhydrite is able to reach to 52.04% after complete free swelling. σ_{max} = 1510 kPa, which indicates that swelling stress under swelling strain inhibited completely of this type anhydrite, is able to reach 1510 kPa. R-square is the coefficient of determination. RMSE (root-mean-square error) is a frequently used measure of the differences between values predicted by a model and the values actually observed. SSE (sum of squares due to error) is used to measure the total deviation of the response values from the fit to the response values. RMSE and SSE values closer to 0 indicate a fit that is more useful for prediction.

temperature field [33]. However, as our model considered the time effect, we used the method of simulating creep for reference to simulate swelling. Our model is essential for describing strain under the effect of stress and time. So with user-defined creep subroutine offered by ANSYS, we can directly simulate swelling.

As shown in Figure 11, based on geologic survey data and design documents of the Lirang tunnel, a 2D finite element model is established using ANSYS. The plane42 element was employed to simulate the surrounding rock, the link1 element was employed to simulate rock bolts, and the beam3 element was employed to simulate first lining. The basic material parameters for both rock stratums and support structure are given in Table 6. As the samples were obtained from the Lirang tunnel, so the parameters listed in Table 5 can be employed for simulating swelling immediately. In this study, we only simulated the process from excavation to the beginning of second lining. Some useful results are presented in Figure 12 and Table 7.

Figures 12(a) and 12(b) show the deformation distribution of surrounding rock on day 36. As shown in Figure 12(a), the arch crowns go down 24.5 cm and the floors are uplifted up to 19.7 cm. It indicates that not only the roof but also the floor of the tunnel are subjected to larger deformation due to the effect of swelling. Figure 12(b) shows that the maximal deformation of surrounding rock is 27.6 cm. Figures 12(c) and 12(d) show the mechanical performance of support structures. As shown in Figure 12(c), the maximal axial force of beam elements on day 36 is 50396 kN coming from arch springing. In the simulation results, the beam elements are mainly subjected to axial force, while both shearing force and bending moment of them are very small. Based on the mechanical performance of beam elements, a maximal compression stress of first lining that is 7.4 MPa is worked out. In Figure 12(d), the maximal axial force of link elements is 197.86 kN, which also comes from the arch springing. Based on the axial force characteristics of link elements, the maximal tensile stress of the rock bolt that is 100.4 MPa was worked out, which is less than the design strength of 130 MPa. Based on the simulation results, we gave some useful and quantitative measures for counteracting the swelling problem:

(a) In consideration that the maximal deformation surrounding the cross section of the tunnel is 27.6 cm, the reserved deformation with 40 cm in thickness was reduced to 30 cm.

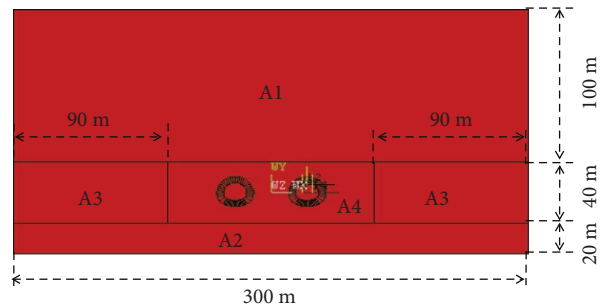

Figure 11: 2D finite model. A1 and A2 are limestone stratums, which are unable to swell. A3 and A4 are anhydrite stratums. A4 is subjected to underground water, so it is able to swell, while A3 is far away from the tunnel and free of underground water, so A3 does not need to consider swelling.

(b) The floor of the tunnel got an upheaval of 19.7 cm, and an overbreak of 20 cm in thickness under the inverted arch was set within laying some gravel as a buffer layer.

(c) As maximal tensile stress of the rock bolt is not beyond the strength tensile, the length and ring direction installation intervals of rock bolts still followed initial design. At the same time, considering that arch springing is subjected to a lager force, we suggested increasing the quantity of rock bolts there when necessary.

The above measures have already been applied to the Lirang tunnel, and a satisfactory result was obtained; especially, the revised reserved deformation provides a scientific basis for cost saving. According to the on-site feedback, the updated reserved deformation is reasonable due to no beyond-limit phenomenon, the measures for the inverted arch are also reasonable due to no upheaval phenomenon, and there was no collapse of surrounding rock and damage to the support structure during the construction period, so such a simulation using ANSYS is able to effectively guide tunneling through anhydrite formation.

5. Discussion

The swelling constitutive model developed in this study is in principle capable of reproducing the swelling behavior of anhydrite as observed in swelling tests. As described in the test method, this model was established under the situation that finite rock is subjected to enough water. However, this is

Table 6: The basic material parameters for both rock stratums and support structure employed for simulation analysis.

Rock stratum	Elasticity modulus (GPa)	Poisson's ratio	Density (g/cm^3)	Friction angle (°)	Cohesive force (MPa)
Limestone	24.50	0.27	2.70	45.28	9.85
Anhydrite	5.00	0.28	2.70	40.00	0.08
Rock bolt	170.00	0.30	7.80	—	—
Initial liner	31.00	0.17	2.50	54.90	3.18

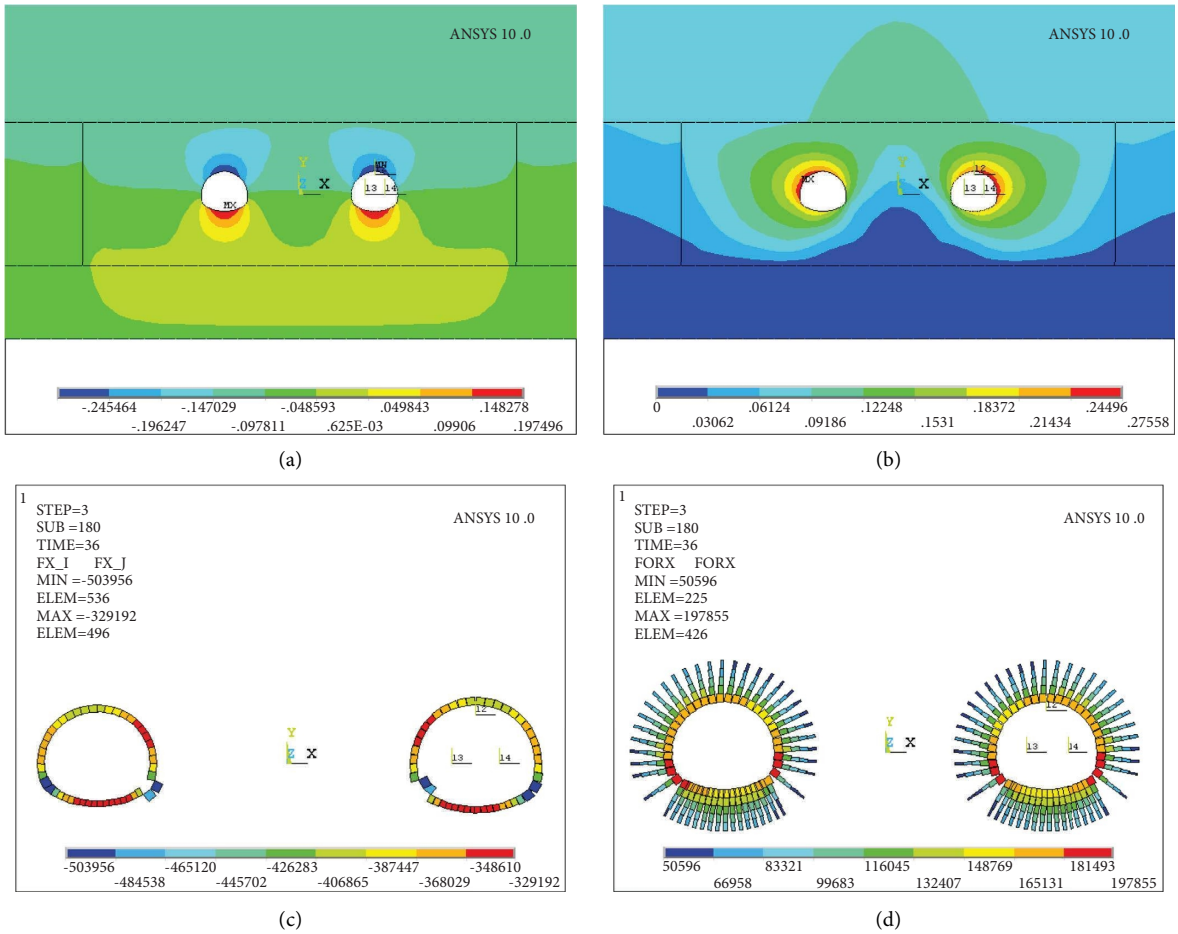

Figure 12: The results of numerical simulation. (a) *Y* direction displacement on day 36 (unit: m). (b) Resultant displacement on day 36 (unit: m). (c) Axial force of first lining on day 36 (unit: m). (d) Axial force of rock bolt on day 36 (unit: m).

Table 7: Summary numerical simulation results using ANSYS.

Crown settlement (cm)	Convergence of wall (cm)	Maximal axial force of LE (kN)	Maximal axial force of LE (kN)	Maximal tensile stress of RB (MPa)	Maximal axial force of BE (kN)	Maximal shearing force of BE (N)	Maximal bending moment of BE (N·m)	Maximal compressive stress of FL (MPa)
24.50	54.00	27.60	197.93	100.4	503.96	1.90	0.30	7.40

Note. SR is surrounding rock. LE is the link1 element. RB is the rock bolt. BE is the beam element. FL is the first lining.

different from a realistic situation that the water content of surrounding rock is different at different positions in the tunnel. In other words, our model is unable to consider the water content of rock, so it is unable to reflect the difference in swelling deformation among different positions in the tunnel due to nonuniform distribution of groundwater. For the above problem, we carry out a further discussion for improving the model in this section.

It is worth noting that after the tunnel is excavated, the surrounding rock of the tunnel will produce cracks, and the groundwater will flow into the tunnel floor along the cracks, causing the tunnel floor to expand significantly.

Existing research supports the view that the main mechanics of anhydrite swelling is the growth of the $CaSO_4{\cdot}2H_2O$ crystal, and the volume swelling strain can be expressed as follows [11, 32]:

$$\frac{d\varepsilon_v}{dt} = \frac{\gamma}{\rho_{DH}} \frac{dm_{DH}}{dt}, \tag{8}$$

where ε_v is the volume-swelling strain, γ is the coefficient which reflects the swelling effect caused by crystal growth, m_{DH} is the water consumed by $CaSO_4{\cdot}2H_2O$ crystal growth, and ρ_{DH} is the density of the $CaSO_4{\cdot}2H_2O$ crystal.

Assuming w is the volumetric water content of anhydrite, based on its definition,

$$\omega = \frac{m_\omega}{m_\gamma}\rho_d, \tag{9}$$

where m_ω is the mass of water in anhydrite rock, m_γ is the drying mass of anhydrite rock, and ρ_d is the rock-drying density.

Taking derivative of equation (9) with respect to time t, then the following equation is obtained:

$$\frac{dm_\gamma}{dt} = \frac{d\omega}{dt}\frac{m_\gamma}{\rho_d}. \tag{10}$$

Assuming that mass change of water in rock is only caused by two reasons, one is that water is consumed by $CaSO_4{\cdot}2H_2O$ crystal growth, set as m_{DH}. The other one is that water loss occurs due to evaporation and diffusion, set as m_l, so the following equation can be obtained:

$$\frac{dm_\gamma}{dt} = \frac{dm_{DH}}{dt} + \frac{dm_l}{dt}. \tag{11}$$

Substituting equations (10) to (11), we obtain

$$\frac{dm_{DH}}{dt} = \frac{d\omega}{dt}\frac{m_\gamma}{\rho_d} - \frac{dm_l}{dt}. \tag{12}$$

Then, substituting equations (12) to (8), we obtain

$$\frac{d\varepsilon_v}{dt} = \frac{\gamma}{\rho_{DH}}\left(\frac{d\omega}{dt}\frac{m_\gamma}{\rho_d} - \frac{dm_l}{dt}\right). \tag{13}$$

A new relationship between swelling strain and time can be obtained by taking the integral of both sides of equation (13) with respect to time:

$$\begin{aligned}\varepsilon_v &= \int_0^t \frac{\gamma}{\rho_{DH}}\left(\frac{d\omega}{dt}\frac{m_\gamma}{\rho_d} - \frac{dm_l}{dt}\right)dt \\ &= \frac{\gamma}{\rho_{DH}}\left(W(t)\frac{m_\gamma}{\rho_d} - L(t)\right),\end{aligned} \tag{14}$$

where $W(t)$ is a function employed to describe volumetric water content changing over time during the swelling process and $L(t)$ is a function employed to describe evaporation and diffusion of water. Equation (14), deduction of which is based on the microcosmic swelling mechanics, considers the mass change of water in rock. However, in this equation, the items $W(t)$ and $L(t)$ are unknown, so we will carry out research on obtaining specific expressions of the two items by using the test method in the follow-up work. After this, a complete expression of ε_v can be obtained. By employing ε_v instead of ε_t in equation (5), a new expression of q is obtained, so that a new swelling constitutive model with consideration of both mass change of water in rock and time is established, and such a model is able to simulate the swelling changing over time at different positions in the tunnel.

Besides, the expansion strain rate of anhydrite is related to the infiltration rate of water in anhydrite for the following reasons: The permeability of anhydrite can not only change the time required for dilatational strain but also affect the stress around gypsum rock, by changing the speed of water immersion in gypsum rock. Thus, the effect of permeability on the expansion stress-strain relationship is a very complex chemical kinetic problem at the mesoscopic level. At this stage, we are committed to solving the tunnel engineering problems related to expansive rock, so from the perspective of phenomenology, we establish a constitutive model whose accuracy meets the requirements of engineering applications. In this constitutive model, the effect of permeability on expansion is attributed and embedded in the change process of the expansion strain with time, which can be embodied by parameters a and b in equation (2).

6. Conclusion

A swelling constitutive model with consideration of the time effect was developed to reproduce the swelling behavior of anhydrite observed in swelling tests. This model is able to describe the dynamic changing of swelling stress-strain of anhydrite in the whole swelling process, so this model can match the construction process of the tunnel with the swelling evolution of surrounding rock, which has practical significance for process simulation and process control of tunnel engineering disaster caused by anhydrite swelling. In addition, by introducing the time effect into the swelling constitutive model, the simulation of swelling can be easily achieved by using the simulation of creep as a reference.

The swelling constitutive model was implemented within ANSYS for the numerical simulation of the Lirang tunnel. This simulation result shows that both the roof and floor of the tunnel are subjected to a larger deformation due to swelling, and arch springing should be paid enough attention. Based on simulation results, some useful measures were proposed and applied to the Lirang tunnel and obtained a satisfactory result according to the feedback information from on-site.

The model developed in this paper is practical enough for solving engineering problems. However, the impossibility of reproducing the swelling deformation difference among different positions in the tunnel reveals that our understanding of swelling influenced by water content is still

incomplete; hence, there is an open field of research in the relationship between water content and swelling of anhydrite.

Data Availability

The data used to support the findings of this study are included within the article.

Disclosure

The manuscript has been submitted as a preprint in the below link [34]: https://www.researchsquare.com/article/rs-1224616/v1.

Conflicts of Interest

The authors declare that they have no conflicts of interest.

Acknowledgments

This work was supported by the Research on Intelligent Prediction Technology of Blasting Vibration of Open-Pit Mine (2022-2-TD-QN006), the National Natural Science Foundation of China (Grant nos. 52208336, 42002249, and 52378332), the Science and Technology Program of Guangzhou Construction Engineering Co., Ltd., Guangzhou, Guangdong 510030, China, the Guangzhou Municipal Construction Group Co., Ltd., Guangzhou, Guangdong 510030, China ((2022)–KJ002, BH20220627543, and (2022)–KJ015), the Guangdong Basic and Applied Basic Research Foundation (2023A1515012826 and 2021A1515011691), and the Science and Technology Projects in Guangzhou (2024A04J3902).

References

[1] C. Butscher, T. Mutschler, and P. Blum, "Swelling of clay-sulfate rocks: a review of processes and controls," *Rock Mechanics and Rock Engineering*, vol. 49, pp. 1–17.

[2] E. E. Alonso, I. R. Berdugo, and A. Ramon, "Extreme expansive phenomena in anhydritic-gypsiferous claystone: the case of Lilla tunnel," *Géotechnique*, vol. 63, no. 7, pp. 584–612, 2013.

[3] Z. Hou, Y. Liu, Z. Han et al., "Experimental study of the bearing characteristics of a novel energy-saving and environmentally friendly pile: drilling with prestressed concrete pipe cased piles," *International Journal of Geomechanics*, vol. 24, no. 4, pp. 1–16, Article ID 4024035, 2024.

[4] G. Anagnostou, *Untersuchungen zur Statik des Tunnelbaus in quellf?higem Gebirge*, vdf Hochschulverlag AG, Zollikon, Switzerland, 1992.

[5] J. Luo, "Gypsumbearing rock group and its effffect on tunnel engineering," *Journal of Southwest Jiaotong University*, vol. 1, pp. 63–72, 1978.

[6] F. Rauh, G. Spaun, and K. Thuro, "Assessment of the swelling potential of anhydrite in tunnelling projects," in *Proceedings of the Pre-Congress Proceedings 10th IAEG Congress*, Nottingham, UK, September 2006.

[7] F. Rauh and K. Thuro, *Investigations on the Swelling Behavior of Pure anhydrites[C]//1st Canada US Rock Mechanics Symposium*, American Rock Mechanics Association, Alexandria, VA, USA, 2007.

[8] B. Sch¨adlich, T. Marcher, and H. F. Schweiger, "Application of a constitutive model for swelling rock to tunnelling," *Geotechnical Engineering*, vol. 44, pp. 47–54, 2013.

[9] G. Anagnostou, E. Pimentel, and K. Serafeimidis, "Swelling of sulphatic claystones – some fundamental questions and their practical relevance," *Geomechanics and Tunnelling*, vol. 3, no. 5, pp. 567–572, 2010.

[10] A. Ramon Tarragona, *Expansion Mechanisms in Sulphated Rocks and Soils*, Alert Geomaterials, Aix-en-Provence, France, 2014.

[11] L. Oldecop and E. Alonso, "Modelling the degradation and swelling of clayey rocks bearing calcium sulphate," *International Journal of Rock Mechanics and Mining Sciences*, vol. 54, pp. 90–102, 2012.

[12] E. Alonso, A. Gens, I. Berdugo, and E. Romero, "Expansive behaviour of a sulphated clay in a railway tunnel," in *Proceedings Of The International Conference On Soil Mechanics And Geotechnical Engineering*, AA BALKEMA PUBLISHERS, Osaka, Japan, September 2005.

[13] I. R. Berdugo, *Tunnelling in Sulphate-Bearing rocksCexpansive Phenomena*, Department of Geotechnical Engineering and Geosciences, Barcelona, Spain, 2007.

[14] Y. Liu, H. Yu, C. Wang, and C. L. Wang, "Research on mechanism of damage of anhydrock in dolomite layer to tunnel structure," *Rock and Soil Mechanics*, vol. 32, no. 9, Article ID 1000C7598, 2010.

[15] E. Fecker, "Influence of swelling rock on tunnelling," *Bulletin of the International Association of Engineering Geology*, vol. 24, no. 1, pp. 27–32, 1981.

[16] K. Serafeimidis and G. Anagnostou, "On the time-development of sulphate hydration in anhydritic swelling rocks," *Rock Mechanics and Rock Engineering*, vol. 46, no. 3, pp. 619–634, 2013.

[17] F. Zhao, L. Zhang, and M. Zhang, "Experimental study on strength characteristics of expansive rock along kunming-nanning railway," *Subgrade Engineering*, vol. 2, p. 21, 2012.

[18] F. Rauh and K. Thuro, *Why Do Pure Anhydrites Diffffer in Their Swelling Capacity?*, ResearchGate, Berlin, Germany, 2006.

[19] Isrm, "Suggested methods for laboratory testing of argillaceous swelling rocks," *International Journal of Rock Mechanics and Mining Sciences*, vol. 26, pp. 415–426, 1989.

[20] F. T. Madsen and M. Muller-Vonmoos, "The swelling behaviour of clays," *Applied Clay Science*, vol. 4, no. 2, pp. 143–156, 1989.

[21] T. T. Kie, *Swelling Rocks and the Stability of Tunnels*, International Society for Rock Mechanics, Lisbon, Portugal, 1983.

[22] E. Pimentel, "Existing methods for swelling tests-A critical review," *Energy Procedia*, vol. 76, pp. 96–105, 2015.

[23] X. Liu, S. Wang, E. Wang, and Q. Xue, "Study on time-dependent swelling constitutive relation of swelling rock," *Journal of Hydraulic Engineering*, vol. 37, no. 2, pp. 195–199, 2006.

[24] R. H. Becker and L. M. Speltz, "Putting the S-curve concept to work," *Research Management*, vol. 26, no. 5, pp. 31–33, 1983.

[25] M. Wittke, "Design, construction, supervision and long-term behaviour of tunnels in swelling rocks," in *Proceedings of the Eurock*, pp. 211–216, London, UK, June 2006.

[26] H. H. Einstein and N. Bischoffff, "Design of tunnels in swelling rock," in *Proceedings of the The 16th US Symposium*

on Rock Mechanics (USRMS), American Rock Mechanics Association, Minneapolis, MN, USA, September 1975.

[27] P. Wittke-Gattermann, "Dimensioning of tunnels in swelling rock," in *Proceedings of the 10th ISRM Congress*, International Society for Rock Mechanics, Sandton, South Africa, September 2003.

[28] H. Grob, *Schwelldruck am Beispiel des Belchentunnels*, Sitzungsberichte Int. Symposium fr Untertagebau, pp 99–119, Luzern, Switzerland, 1972.

[29] O. J. Pejon and L. V. Zuquette, "Effects of strain on the swelling pressure of mudrocks," *International Journal of Rock Mechanics and Mining Sciences*, vol. 43, no. 5, pp. 817–825, 2006.

[30] K. Kovari, F. T. Madsen, and C. Amstad, "Tunnelling with yielding support in swelling rocks," in *Proceedings of the ISRM International Symposium*, International Society for Rock Mechanics, Tokyo, Japan, September 1981.

[31] Y. Xie, C. Zheng-han, S.-G. Sun, and G. Li, "Test research on three-dimensional swelling pressure of remolded expansive clay," *Rock and Soil Mechanics*, vol. 28, no. 8, pp. 1636–1642, 2007.

[32] A. A. Jeschke, K. Vosbeck, and W. Dreybrodt, "Surface controlled dissolution rates of gypsum in aqueous solutions exhibit nonlinear dissolution kinetics," *Geochimica et Cosmochimica Acta*, vol. 65, no. 1, pp. 27–34, 2001.

[33] X. Miao, "Large deformation analysis of surrounding rock of a tunnel in swelling rock mass based on the humidity stress fifield theory," *Journal of China University of Mining and Technology*, vol. 24, no. 1, pp. 58–63, 1995.

[34] Z. Hou and J. Wu, "A practical swelling constitutive model of anhydrite and its application on tunnel engineering," *Research Square*, 2022.